

# Degradation and modification of metallaboranes. Part 4: Synthesis and characterization of a series of hybrid bimetallaborane clusters of the type $[2,2,2-(\text{PPh}_3)_2(\text{CO})\text{-nido-2-OsB}_4\text{H}_7\text{-3-(BH}_2\text{PPh}_2)\text{C}_x\text{H}_y\text{PPh}_2\text{RuCl}_2(p\text{-cym)}]$

Paul McQuade, Rudolph E.K. Winter, Nigam P. Rath, Lawrence Barton \*

Department of Chemistry, Biochemistry and the Center for Molecular Electronics, University of Missouri – St. Louis, St. Louis, MO 63121, USA

Received 6 August 2004; accepted 4 October 2004

Available online 28 October 2004

This paper is dedicated to a nice man, Professor F. Gordon A. Stone in honor of his 80th birthday and a career which defined organometallic chemistry

## Abstract

Reactions between a series bidentate phosphines, with the general formula  $\text{PPh}_2(\text{CH}_2)_n\text{PPh}_2$ , and the air stable hexaborane(10) analogue  $[2,2,2-(\text{PPh}_3)_2(\text{CO})\text{-nido-2-OsB}_5\text{H}_9]$  (**1**), afford species of the type  $\{[(\text{PPh}_3)_2(\text{CO})\text{OsB}_4\text{H}_7]\text{-3-}\{(\text{BH}_2\text{PPh}_2(\text{CH}_2)_n(\text{PPh}_2))\}\}$  (**2**) which contain a pendent  $\text{PPh}_2$  group. In solution **2** can undergo an intramolecular substitution reaction to form the species  $\{[(\text{PPh}_3)(\text{CO})\text{OsB}_4\text{H}_7]\text{-}\eta^2\text{-3,2-}\{(\text{BH}_2\text{PPh}_2(\text{CH}_2)_n(\text{PPh}_2))\}\}$  (**4**). In spite of this, chemistry at the pendent  $\text{PPh}_2$  group may be studied and herein are reported the results of reactions of **2** with the organometallic reagent  $[(p\text{-cym})\text{RuX}_2]_2$  ( $\text{X} = \text{Cl, I}$ ) to afford hybrid bimettallaborane clusters of the type  $[2,2,2-(\text{PPh}_3)_2(\text{CO})\text{-nido-2-OsB}_4\text{H}_7\text{-3-(BH}_2\text{PPh}_2)\text{C}_x\text{H}_y\text{PPh}_2\text{RuCl}_2(p\text{-cym)}]$  (**5**). The species obtained include  $[2,2,2-(\text{PPh}_3)_2(\text{CO})\text{-nido-2-OsB}_4\text{H}_7\text{-3-(BH}_2\text{-dppp}\cdot\text{Ru}(p\text{-cym})\text{Cl}_2)]$  (**5a**),  $[2,2,2-(\text{PPh}_3)_2(\text{CO})\text{-nido-2-OsB}_4\text{H}_7\text{-3-(BH}_2\text{-dppp}\cdot\text{Ru}(p\text{-cym})\text{Cl}_2)]$  (**5b**),  $[2,2,2-(\text{PPh}_3)_2(\text{CO})\text{-nido-2-OsB}_4\text{H}_7\text{-3-(BH}_2\text{-dpph}\cdot\text{Ru}(p\text{-cym})\text{Cl}_2)]$  (**5c**),  $[2,2,2-(\text{PPh}_3)_2(\text{CO})\text{-nido-2-OsB}_4\text{H}_7\text{-3-(BH}_2\text{-dppx}\cdot\text{Ru}(p\text{-cym})\text{Cl}_2)]$  (**5d**) and  $[2,2,2-(\text{PPh}_3)_2(\text{CO})\text{-nido-2-OsB}_4\text{H}_7\text{-3-(BH}_2\text{-dppp}\cdot\text{Ru}(p\text{-cym})\text{I}_2)]$  (**6**). Species **5d** was also prepared from the reaction between **1** and the known compound  $[\text{dppx}\cdot\text{Ru}(p\text{-cym})\text{Cl}_2]$ . Species **5a–5d** and **6** were characterized by elemental analysis, high resolution mass spectrometry and NMR spectrometry; the latter affording some novel features for this series of compounds. Structure determination by X-ray diffraction was not successful but a structure of the analogue  $[\text{BH}_3\cdot(\text{PPh}_2)(\text{CH}_2)_6(\text{PPh}_2)\cdot\text{Ru}(p\text{-cym})\text{Cl}_2]$  (**7**) is reported.

© 2004 Elsevier B.V. All rights reserved.

**Keywords:** Boron hydrides; Metallaboranes; Ruthenium; Phosphines; NMR spectroscopy

## 1. Introduction

We recently described reactions of bidentate bases with the metallahexaborane  $[2,2,2-(\text{PPh}_3)_2(\text{CO})\text{-nido-OsB}_5\text{H}_9]$  (**1**) [1]. Such reactions between small metallaboranes and bidentate bases have not received much attention, although reactions with simple bases have attracted increased interest in recent years [2]. These reaction with base might be expected to lead to adducts with more open structures [3], however they actually tend to proceed either by degradation of the cluster framework or by initial rearrangement of the cluster followed by degradation. An example of this is given in Scheme 1,

\* Corresponding author. Tel.: +3145265334; fax: +3145165342.

E-mail address: lbarton@umsl.edu (L. Barton).

which shows the reactions of bidentate phosphines with **1** and subsequent rearrangement of the product [1a]. In this reaction one end of the ligand attaches to one of the basal boron atoms in the cage and, after rearrangement, the phosphine moiety remains attached to an exopolyhedral BH<sub>2</sub> group bonded to a basal boron atom in an osmapentaborane cage. The other end of the phosphine ligand remains uncoordinated and is therefore amenable to further chemistry. This process, which has been shown to be reversible, forms species of the type [2,2,2-(PPh<sub>3</sub>)<sub>2</sub>(CO)-*nido*-2-OsB<sub>4</sub>H<sub>7</sub>-3-(BH<sub>2</sub>·PPh<sub>2</sub>C<sub>x</sub>H<sub>y</sub>P-Ph<sub>2</sub>)] (**2**) from **1**. Further chemistry may occur involving loss of phosphine–borane to afford the lower homologue species [2,2,2-(PPh<sub>3</sub>)<sub>2</sub>(CO)-*nido*-2-OsB<sub>4</sub>H<sub>8</sub>] (**3**) or intramolecular substitution to form products of type **4**, as shown in Scheme 1. The latter species [{(PPh<sub>3</sub>)(CO)OsB<sub>4</sub>H<sub>7</sub>}-η<sup>2</sup>-3,2-{BH<sub>2</sub>PPh<sub>2</sub>(CH<sub>2</sub>)<sub>n</sub>(PPh<sub>2</sub>)}] (**4**) is formed by replacement of a PPh<sub>3</sub> group on Os by the pendant PPh<sub>2</sub> group on the cage and its formation may be precluded by the use of bidentate phosphines with less flexible backbones [1c]. However, chemistry may be conducted at the pendent PPh<sub>2</sub> group, as we demonstrated previously [1a], and this paper describes the formation of some hybrid systems, one of which is illustrated in Fig. 1, either by direct reaction with species of type **2** or by reaction of mono-functionalized bidentate phosphines with **1**.

## 2. Experimental

### 2.1. General procedures

Volatile materials were manipulated using a standard high vacuum line, and dry box techniques were used for

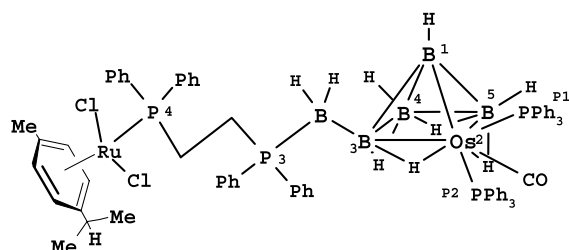
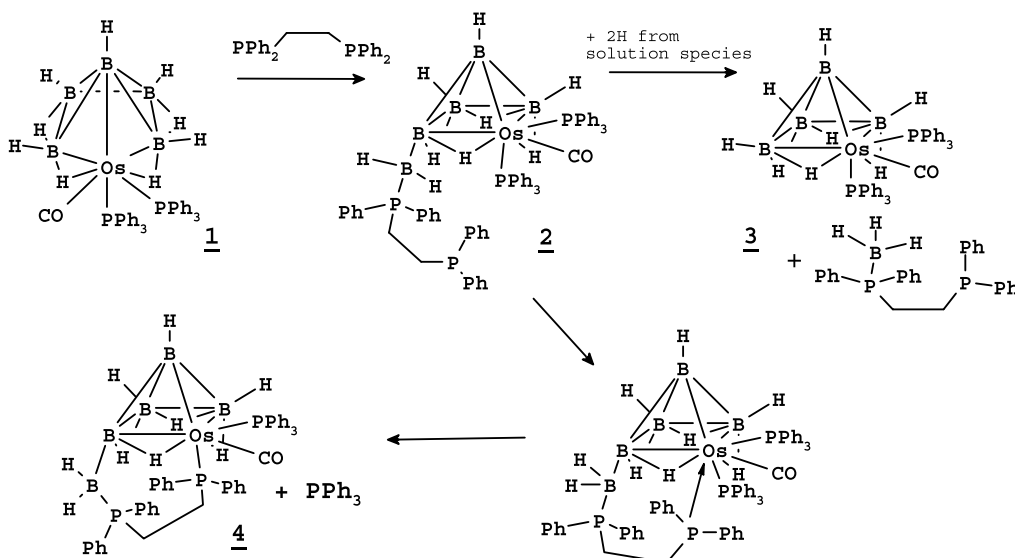


Fig. 1. Proposed structure for [2,2,2-(PPh<sub>3</sub>)<sub>2</sub>(CO)-*nido*-2-OsB<sub>4</sub>H<sub>7</sub>-3-(BH<sub>2</sub>·dppe·Ru(*p*-cym)Cl<sub>2</sub>)] (**5a**) showing the numbering system.

nonvolatile air sensitive materials [4]. Solvents used were reagent grade and were dried before use. Products were isolated by radial chromatography (Harrison Research, Palo Alto, CA) under a dry N<sub>2</sub> atmosphere using a 25 cm diameter circular plate coated with 0.1 cm of silica gel (EM Science), made from aqueous slurries followed by drying at 70 °C. NMR spectroscopy was carried out on a Bruker ARX 500 spectrometer operating at 500.1 MHz for proton, 160.5 MHz for boron-11, and at 202.5 MHz for phosphorus-31 and on a Varian Unity Plus 300 spectrometer operating at 96.2 MHz for <sup>11</sup>B, 299.9 MHz for <sup>1</sup>H and 121.4 MHz for <sup>31</sup>P nuclei. Chemical shifts are reported in ppm for CDCl<sub>3</sub> solutions, unless otherwise stated, to low field (high frequency) of Et<sub>2</sub>O·BF<sub>3</sub> for <sup>11</sup>B, of SiMe<sub>4</sub> for <sup>1</sup>H and of 85% H<sub>3</sub>PO<sub>4</sub> for <sup>31</sup>P. Mass spectra were measured on a JEOL MStation JMS700 and elemental analyses were carried out by Atlantic Microlabs Inc., Norcross, GA.

### 2.2. Starting materials and reagents

B<sub>5</sub>H<sub>9</sub> was obtained from laboratory stock, and distilled on a high vacuum line before use. [2,2,2-



Scheme 1.

$(\text{PPh}_3)_2(\text{CO})\text{-nido-2-OsB}_5\text{H}_9$  (**1**) was prepared according to the literature method [5]. 1,4-Dibromo benzene (Eastman Organic) was used as received and  $\alpha,\alpha'$ -dibromo-*p*-xylene (Eastman) was sublimed before use.  $\text{RuCl}_3 \cdot \text{XH}_2\text{O}$  (Alfa) and *R*(-)- $\alpha$ -Phellandren  $\text{C}_{10}\text{H}_{16}$  (Fluka) were used as received. The phosphines  $[(\text{PPh}_2)_2(\text{CH}_2)_3]$  (dppp), obtained from Strem,  $[(\text{PPh}_2)_2(\text{CH}_2)_3]$  (dppe) and  $[(\text{PPh}_2)_2(\text{CH}_2)_6]$  (dpph), both obtained from Aldrich, were used as received.  $[\text{PPh}_2\text{CH}_2\text{C}_6\text{H}_4\text{CH}_2\text{PPh}_2]$  (dppx) [6] was prepared according to literature methods and  $\text{PPh}_2\text{CH}_2\text{C}_6\text{H}_4\text{CH}_2\text{PPh}_2 \cdot \text{Ru}(p\text{-cym})\text{Cl}_2$  {dppx· $\text{Ru}(p\text{-cym})\text{Cl}_2$ } as described previously [7] from dppx and  $[\text{Ru}(p\text{-cym})\text{Cl}_2]_2$ . The latter was prepared from  $\text{RuCl}_3 \cdot \text{XH}_2\text{O}$  and *R*(-)- $\alpha$ -Phellandren [8] and  $[\text{Ru}(p\text{-cym})\text{I}_2]_2$  was prepared by adding NaI to a saturated aqueous solution of  $[\text{Ru}(p\text{-cym})\text{Cl}_2]_2$  [9].  $[(\text{PPh}_3)_2(\text{CO})\text{OsB}_4\text{H}_7\text{-3-(BH}_2 \cdot \text{dppe)}]$  (**2a**) and  $[(\text{PPh}_3)_2(\text{CO})\text{OsB}_4\text{H}_7\text{-3-(BH}_2 \cdot \text{dppp)}]$  (**2b**) [1a], and  $[(\text{PPh}_3)_2(\text{CO})\text{OsB}_4\text{H}_7\text{-3-(BH}_2 \cdot \text{dppx)}]$  (**2d**) [1c] were prepared as described previously.

### 2.3. Preparation of $[2,2,2\text{-}(\text{PPh}_3)_2(\text{CO})\text{-nido-2-OsB}_4\text{H}_7\text{-3-(BH}_2 \cdot \text{dppe} \cdot \text{Ru}(p\text{-cym})\text{Cl}_2)]$ (**5a**), $[2,2,2\text{-}(\text{PPh}_3)_2(\text{CO})\text{-nido-2-OsB}_4\text{H}_7\text{-3-(BH}_2 \cdot \text{dppp} \cdot \text{Ru}(p\text{-cym})\text{Cl}_2)]$ (**5b**) and $[2,2,2\text{-}(\text{PPh}_3)_2(\text{CO})\text{-2-nido-OsB}_4\text{H}_7\text{-3-(BH}_2 \cdot \text{dpph} \cdot \text{Ru}(p\text{-cym})\text{Cl}_2)]$ (**5c**)

The procedures and results for **5a**, **5b** and **5c** were very similar so details are only given for **5a**. A one necked 50 mL round bottom flask containing a stir bar was charged with 52 mg (0.065 mmol) of  $(\text{PPh}_3)_2(\text{CO})\text{OsB}_5\text{H}_9$  and 80 mg (0.20 mmol) of dppe. Freshly distilled  $\text{CH}_2\text{Cl}_2$  (20 mL), was added and the solution stirred for 12 h. at room temperature. 150 mg (0.25 mmol) of  $[\text{Ru}(p\text{-cym})\text{Cl}_2]_2$  was then added and the solution stirred for a further 10 min. After concentrating the solution to 1 mL, it was applied to the radial chromatograph using  $\text{CH}_2\text{Cl}_2$  as the mobile phase. A single fraction was obtained which gave a yellow solution containing  $(\text{PPh}_3)_2(\text{CO})\text{OsB}_4\text{H}_8$  (**3**) and  $[2,2,2\text{-}(\text{PPh}_3)(\text{CO})\text{-nido-2-OsB}_4\text{H}_7\text{-3,2-(BH}_2 \cdot \text{dppe)}]$  (**4**).  $\text{PPh}_3$  was also present in this fraction, and is formed in the conversion of  $[2,2,2\text{-}(\text{PPh}_3)_2(\text{CO})\text{-nido-2-OsB}_4\text{H}_7\text{-3-(BH}_2 \cdot \text{dppe)}]$  **2a** to  $[2,2\text{-}(\text{PPh}_3)(\text{CO})\text{-nido-2-OsB}_4\text{H}_7\text{-3,2-(BH}_2 \cdot \text{dppe)}]$  **4a**, illustrated in Scheme 1.<sup>1</sup> A trace amount of  $[2,2,2\text{-}(\text{PPh}_3)_2(\text{CO})\text{-nido-2-OsB}_4\text{H}_7\text{-3-(BH}_2 \cdot \text{PPh}_3)]$  was also observed produced by subsequent reaction of  $\text{PPh}_3$  with  $(\text{PPh}_3)_2(\text{CO})\text{OsB}_5\text{H}_9$  [1a,2a].  $\text{CH}_3\text{CN}$  was then slowly added to the eluent until a red band was detected. The red solution obtained from this band was reduced to dryness on a rotary evaporator giving 32 mg (33% yield based on

$[(\text{PPh}_3)_2(\text{CO})\text{OsB}_5\text{H}_9]$  of a red solid which was characterized as  $[2,2,2\text{-}(\text{PPh}_3)_2(\text{CO})\text{-nido-2-OsB}_4\text{H}_7\text{-3-(BH}_2 \cdot \text{dppe} \cdot \text{Ru}(p\text{-cym})\text{Cl}_2)]$  (**5a**). Attempts to grow crystals of **5a** suitable for X-ray diffraction were unsuccessful; generally these attempts produced only amorphous red spheres. The methods employed included slow diffusion of  $\text{C}_6\text{H}_{14}$  into a  $\text{C}_6\text{H}_6/\text{CH}_2\text{Cl}_2$  solution containing **5a** at 5 °C, slow diffusion of  $\text{Et}_2\text{O}$  into a  $\text{CDCl}_3$  solution containing **5a** at -20 °C. In addition to these methods slow evaporation of a  $\text{CH}_2\text{Cl}_2/\text{C}_6\text{H}_{14}$  solution of **5a** at -20 °C was also attempted. Crystallization experiments had to be carried out at lowered temperature due to the slow degradation of **5a** in solution at room temperature, and we ascribed this slow degradation as the reason for our inability to obtain crystal structures of the hybrid clusters.  $^1\text{H}$  NMR ( $\text{CDCl}_3$ ): *p*-cymene, ( $\delta$  in ppm) 0.96 (d,  $J = 7.04$  Hz, 3H,  $\text{CHMe}_2$ ), 0.93 (d,  $J = 7.02$  Hz, 3H,  $\text{CHMe}_2$ ), 1.80 (s, 3H, *Me*), 2.52 (sept,  $J = 6.95$  Hz, 1H,  $\text{CHMe}_2$ ), 4.99 (d,  $J = 5.93$  Hz, 1H,  $\text{MeC}_6\text{H}_4\text{CHMe}_2$ ), 5.14 (d,  $J = 6.05$  Hz, 1H,  $\text{MeC}_6\text{H}_4\text{CHMe}_2$ ), 5.19 (overlapping pair of d, 2H,  $\text{MeC}_6\text{H}_4\text{CHMe}_2$ );  $\text{PPh}_2\text{CH}_2\text{CH}_2\text{PPh}_2$ , ( $\delta$  in ppm) 2.85 (m, 2H,  $\text{CH}_2\text{PPh}_2 \cdot \text{Ru}(p\text{-cym})\text{Cl}_2$ ), 2.34 (m, 2H,  $\text{BH}_2 \cdot \text{PPh}_2\text{CH}_2$ ), 6.96–7.81 (m, 50H, Ph, this also includes Phenyl protons on  $\text{PPh}_3$  groups which are coordinated to Os center). The remaining  $^1\text{H}$  data along with  $^{31}\text{P}$  and  $^{11}\text{B}$  can be found in Table 1 [10]. Elemental Anal.: **5a** for  $\text{C}_{73}\text{H}_{77}\text{B}_5\text{P}_4\text{Cl}_2\text{O}_1\text{Os}_1\text{Ru}_1$ , Calc. C, 58.05; H, 5.14. Found: C, 57.68; H, 5.21%. LRMS: FAB (3-NBA and CsI). Calc. for  $^{12}\text{C}_{73}^{1}\text{H}_{77}^{11}\text{B}_4^{10}\text{B}_1^{31}\text{P}_2^{35}\text{Cl}_2^{16}\text{O}_1^{192}\text{Os}_1^{102}\text{Ru}_1^{133}\text{Cs}_1$   $[\text{M} + \text{Cs}]^+$  1644.25, obs. 1644 [11]. The mass envelope for the observed spectrum for **5a** matches that calculated from known isotopic abundances of the constituent elements and is given as supplementary material.

37 mg (43% yield based on  $[(\text{PPh}_3)_2(\text{CO})\text{OsB}_5\text{H}_9]$  of the red solid  $[(\text{PPh}_3)_2(\text{CO})\text{OsB}_4\text{H}_7\text{-3-(BH}_2 \cdot \text{dppp} \cdot \text{Ru}(p\text{-cym})\text{Cl}_2)]$  (**5b**) was obtained in a similar process using 45 mg (0.56 mmol) **1**, 90 mg (0.22 mmol) dppp and 160 mg (0.26 mmol)  $[\text{Ru}(p\text{-cym})\text{Cl}_2]_2$ . Again extensive attempts to grow crystals suitable for X-ray analysis were unsuccessful.  $^1\text{H}$  NMR ( $\text{CDCl}_3$ ): *p*-cymene, ( $\delta$  in ppm) 0.76 (d,  $J = 6.87$  Hz, 3H,  $\text{CHMe}_2$ ), 0.75 (d,  $J = 6.99$  Hz, 3H,  $\text{CHMe}_2$ ), 1.82 (s, 3H, *Me*), 2.50 (m, 1H,  $\text{CHMe}_2$ ), 5.04 (d,  $J = 6.01$  Hz, 1H,  $\text{MeC}_6\text{H}_4\text{CHMe}_2$ ), 5.02 (d,  $J = 5.96$  Hz, 1H,  $\text{MeC}_6\text{H}_4\text{CHMe}_2$ ), 5.21 (d,  $J = 5.68$  Hz, 2H,  $\text{MeC}_6\text{H}_4\text{CHMe}_2$ );  $\text{PPh}_2\text{CH}_2\text{CH}_2\text{CH}_2\text{PPh}_2$ , ( $\delta$  in ppm) 2.66 (m, 1H,  $\text{CH}_2\text{PPh}_2 \cdot \text{Ru}(p\text{-cym})\text{Cl}_2$ ), 2.50 (m, 1H,  $\text{CH}_2\text{PPh}_2 \cdot \text{Ru}(p\text{-cym})\text{Cl}_2$ ), 1.34 (m, 1H,  $\text{CH}_2\text{CH}_2\text{CH}_2$ ), 1.22 (m, 1H,  $\text{CH}_2\text{CH}_2\text{CH}_2$ ) 2.16 (m, 1H,  $\text{BH}_2 \cdot \text{PPh}_2\text{CH}_2$ ), 2.07 (m, 1H,  $\text{BH}_2 \cdot \text{PPh}_2\text{CH}_2$ ), 6.92–7.79 (m, 50H, Ph). The remaining NMR data are listed in Table 1. Elemental Anal.: **5b** for  $\text{C}_{74}\text{H}_{79}\text{B}_5\text{P}_4\text{Cl}_2\text{O}_1\text{Os}_1\text{Ru}_1$ , Calc. C, 58.30; H, 5.22. Found: C, 56.43; H, 5.78%. LRMS: FAB (3-NBA and CsI). Calc. for  $^{12}\text{C}_{74}^{1}\text{H}_{79}^{11}\text{B}_4^{10}\text{B}_1^{31}\text{P}_2^{35}\text{Cl}_2^{16}\text{O}_1^{192}\text{Os}_1^{102}\text{Ru}_1^{133}\text{Cs}_1$   $[\text{M} + \text{Cs}]^+$  1658.27, obs. 1658.

<sup>1</sup> Identified from NMR spectra. See reference [10].

Table 1

$^{11}\text{B}$ ,  $^1\text{H}$  and  $^{31}\text{P}$  NMR ( $\delta$  in ppm) data for [2,2,2-( $\text{PPh}_3$ ) $_2$ (CO)-*nido*-2-OsB $_4$ H $_7$ -3-(BH $_2$ ·dppe·Ru(*p*-cym)Cl $_2$ )] (**5a**), [2,2,2-( $\text{PPh}_3$ ) $_2$ (CO)-*nido*-2-OsB $_4$ H $_7$ -3-(BH $_2$ ·dppp·Ru(*p*-cym)Cl $_2$ )] (**5b**), [2,2,2-( $\text{PPh}_3$ ) $_2$ (CO)-*nido*-2-OsB $_4$ H $_7$ -3-(BH $_2$ ·dppe·Ru(*p*-cym)Cl $_2$ )] (**5c**), [2,2,2-( $\text{PPh}_3$ ) $_2$ (CO)-*nido*-2-OsB $_4$ H $_7$ -3-(BH $_2$ ·dppx·Ru(*p*-cym)Cl $_2$ )] (**5d**) and [2,2,2-( $\text{PPh}_3$ ) $_2$ (CO)-*nido*-2-OsB $_4$ H $_7$ -3-(BH $_2$ ·dppe·Ru(*p*-cym)I $_2$ )] (**6**)

Species	[Compound <b>5a</b> ] <sup>a</sup>		[Compound <b>5b</b> ] <sup>a</sup>		[Compound <b>5c</b> ] <sup>a</sup>		[Compound <b>5d</b> ] <sup>a</sup>		[Compound <b>6</b> ] <sup>a</sup>	
Mode/atom	$^{31}\text{P}\{^1\text{H}\}$		$^{31}\text{P}\{^1\text{H}\}$		$^{31}\text{P}\{^1\text{H}\}$		$^{31}\text{P}\{^1\text{H}\}$		$^{31}\text{P}\{^1\text{H}\}$	
P(2) <sup>b</sup>	+13.85m		+13.58t $J = 9.84$ Hz		+13.93quint $J = 9.70$ Hz		+13.88t $J = 10.59$ Hz		+13.91m	
P(1) <sup>b</sup>	+9.86d $J = 8.36$ Hz		+8.66d $J = 9.86$ Hz		+9.10d $J = 8.56$ Hz		+9.15d $J = 9.86$ Hz		+9.50d $J = 9.41$ Hz	
P(3)	+22.28br <sup>c</sup>		+18.48br		+18.81br		+22.67br		+23.45d $J = 27.25$ Hz	
P(4)	+22.28br <sup>c</sup>		+23.98d $J = 1.90$ Hz		+24.05s		+29.06d $J = 4.88$ Hz		+18.00d $J = 31.38$ Hz	
Mode/atom	$^{11}\text{B}$	$^1\text{H}\{^{11}\text{B}\}$	$^{11}\text{B}$	$^1\text{H}\{^{11}\text{B}\}$	$^{11}\text{B}$	$^1\text{H}\{^{11}\text{B}\}$	$^{11}\text{B}$	$^1\text{H}\{^{11}\text{B}\}$	$^{11}\text{B}$	$^1\text{H}\{^{11}\text{B}\}$
<b>4</b>	+8.95	+5.27	+9.18	+5.33	+8.53	+5.33	+8.14	+5.30	+8.27	+5.34
<b>3</b>	+8.95	<sup>d</sup>	9.18	<sup>d</sup>	8.53	<sup>d</sup>	+8.14	<sup>d</sup>	+8.27	<sup>d</sup>
<b>5</b>	-16.20	+1.16	-15.95	+1.26	-16.47	+1.10	-14.98	+1.23	15.35	+1.21
<b>1</b>	-29.10	+0.087	-29.54	-0.040	-30.05	+0.018	-29.41	-0.13	29.29	+0.00
<b>6',6</b>	-38.03	+1.43, +1.55	-38.65	+1.44, +1.29	-38.30	+1.39, +1.59	-36.55	+1.33, +1.52	-37.76	+1.58, +1.44
H(3,4)		-1.67		-1.82		-1.71		-1.57		-1.65
H(4,5)		-2.36		-2.40		-2.31		-2.32		-2.32
H(2,5)		-10.41		-10.41		-10.45		-10.39		-10.41
H(2,3) <sup>e</sup>		-9.36d $J = 41.01$ Hz		-9.55d $J = 45.01$ Hz		-9.18d $J = 41.67$ Hz		-9.24d $J = 42.01$ Hz		-9.37d $J = 43.11$ Hz

<sup>a</sup> CDCl $_3$ , 298 K.

<sup>b</sup> P(2) is coupling with both P(1) and P(3). P(1) is only coupling with P(2).

<sup>c</sup> Signals due to P(3) and P(4) overlap.

<sup>d</sup> Site of BH $_2$ (PPh $_2$ ) substituent.

<sup>e</sup> Doublets due to  $^2J(^{31}\text{P}-^1\text{H})$  *trans* coupling.

Additional mass spectral data for **5b** are given as supplementary material.

Similarly 23 mg (47% yield) of **5c** was obtained from the reaction of 25 mg (0.031 mmol) of **1** with 100 mg (0.22 mmol) of dpph and 165 mg (0.27 mmol) of freshly prepared  $[\text{Ru}(p\text{-cym})\text{Cl}_2]_2$ . The resulting product mixture was worked up as described for **5a** to afford the red solid  $[2,2,2\text{-}(\text{PPh}_3)_2(\text{CO})\text{-nido-2-OsB}_4\text{H}_7\text{-3-(BH}_2\cdot\text{dpph}\cdot\text{Ru}(p\text{-cym})\text{Cl}_2)]$  (**5c**). Again attempts to produce crystals suitable for X-ray diffraction proved unsuccessful.  $^1\text{H}$  NMR ( $\text{CDCl}_3$ ): *p*-cymene, ( $\delta$  in ppm) 0.78 (d,  $J = 6.89$  Hz, 3H,  $\text{CHMe}_2$ ), 0.77 (d,  $J = 6.81$  Hz, 3H,  $\text{CHMe}_2$ ), 1.92 (s, 3H, *Me*), 2.52 (sept,  $J = 6.96$  Hz, 1H,  $\text{CHMe}_2$ ), 5.06 (m, 2H,  $\text{MeC}_6\text{H}_4\text{CHMe}_2$ ), 5.24 (d,  $J = 5.62$  Hz, 2H,  $\text{MeC}_6\text{H}_4\text{CHMe}_2$ );  $\text{PPh}_2(\text{CH}_2)_6\text{PPh}_2$ , ( $\delta$  in ppm) 2.42 (m, 2H,  $\text{CH}_2\text{PPh}_2\cdot\text{Ru}(p\text{-cym})\text{Cl}_2$ ), 0.90 (m, 2H,  $\text{CH}_2\text{CH}_2\text{PPh}_2\cdot\text{Ru}(p\text{-cym})\text{Cl}_2$ ), 1.00–1.42 (m, 6H,  $\text{CH}_2\text{CH}_2\text{CH}_2\text{CH}_2\text{CH}_2\text{CH}_2$ ), 2.22 (m, 1H,  $\text{BH}_2\cdot\text{PPh}_2\text{CH}_2$ ), 1.95 (m, 1H,  $\text{BH}_2\cdot\text{PPh}_2\text{CH}_2$ ), 6.95–7.91 (m, 50H, Ph). The remaining NMR data are found in Table 1. Elemental Anal.: **5c** for  $\text{C}_{77.5}\text{H}_{86}\text{B}_5\text{P}_4\text{Cl}_3\text{O}_1\text{Os}_1\text{Ru}_1$ , i.e., **5c** containing 0.5 moles  $\text{CH}_2\text{Cl}_2$ , Calc. C, 57.85; H, 5.39. Found: C, 57.40; H, 5.44%. LRMS: FAB (3-NBA and CsI). Calc. for  $^{12}\text{C}_{77}\text{H}_{85}\text{B}_4\text{B}_1\text{P}_2\text{P}_2\text{Cl}_2\text{O}_1\text{Os}_1\text{Ru}_1\text{Cs}_1$  [ $\text{M} + \text{Cs}$ ] $^+$  1700.31, obs. 1700. Additional mass spectral data for **5c** are given in Table 3 in the supplementary material.

#### 2.4. Preparation of $[2,2,2\text{-}(\text{PPh}_3)_2(\text{CO})\text{-nido-2-OsB}_4\text{H}_7\text{-3-(BH}_2\cdot\text{dppx}\cdot\text{Ru}(p\text{-cym})\text{Cl}_2)]$ (**5d**)

To a 50 mL 2-necked round bottom flask containing 45 mg (0.056 mmol) of  $(\text{PPh}_3)_2(\text{CO})\text{OsB}_5\text{H}_9$  in the dry box was added 100 mg (0.21 mmol) of dppx. 20 mL of  $\text{CH}_2\text{Cl}_2$  was added on the vacuum line and the mixture stirred at ambient temperature for 12 h. Then 160 mg (0.22 mmol) of  $[\text{Ru}(p\text{-cym})\text{Cl}_2]_2$  was added under  $\text{N}_2$  flow and the mixture was stirred for 10 min. during which time a brown precipitate formed. Exposure to air and filtration through a 1 cm plug of celite afforded a red clear solution. The solution was then concentrated to 1 mL under reduced pressure and applied to the radial chromatograph using  $\text{CH}_2\text{Cl}_2$  as the mobile phase. The single fraction initially obtained gave a yellow solution which proved to be  $[(\text{PPh}_3)_2(\text{CO})\text{OsB}_4\text{H}_8]$  along with traces of phosphine boranes. Slow elution with  $\text{CH}_3\text{CN}$  allowed isolation of a red band which afforded 41 mg (46% yield based on  $[(\text{PPh}_3)_2(\text{CO})\text{OsB}_5\text{H}_9]$ ) of a red solid that was characterized as  $[2,2,2\text{-}(\text{PPh}_3)_2(\text{CO})\text{-nido-2-OsB}_4\text{H}_7\text{-3-(BH}_2\cdot\text{dppx}\cdot\text{Ru}(p\text{-cym})\text{Cl}_2)]$  (**5d**). Attempts to grow crystals suitable for X-ray diffraction again proved unsuccessful.  $^1\text{H}$  NMR ( $\text{CDCl}_3$ ): *p*-cymene, ( $\delta$  in ppm) 0.87 (apparent t,  $J = 6.67$  Hz, 6H,  $\text{CHMe}_2$ ), 1.81 (s, 3H, *Me*), 2.48 (sept,  $J = 6.67$  Hz, 1H,  $\text{CHMe}_2$ ), 5.11 (m, 2H,  $\text{MeC}_6\text{H}_4\text{CHMe}_2$ ), 5.23 (m, 2H,  $\text{MeC}_6\text{H}_4\text{CHMe}_2$ );  $\text{PPh}_2\text{CH}_2\text{C}_6\text{H}_4\text{PPh}_2$ , ( $\delta$  in ppm)

3.42 (m, 1H,  $\text{BH}_2\cdot\text{PPh}_2\text{CH}_2$ ), 3.66 (m, 1H,  $\text{BH}_2\cdot\text{PPh}_2\text{CH}_2$ ), 3.83 (d,  $^2J_{\text{H-P}} = 8.96$  Hz,  $\text{CH}_2\text{PPh}_2\cdot\text{Ru}(p\text{-cym})\text{Cl}_2$ ), 6.11 (d,  $J = 7.58$  Hz,  $\text{CH}_2\text{C}_6\text{H}_4\text{CH}_2$ ), 6.39 (11 (d,  $J = 7.58$  Hz,  $\text{CH}_2\text{C}_6\text{H}_4\text{CH}_2$ )), 7.02–7.82 (m, 50H, Ph). The remaining  $^1\text{H}$  data along with  $^{31}\text{P}$  and  $^{11}\text{B}$  can be found in Table 1. Elemental Anal.: **5d** for  $\text{C}_{79}\text{H}_{81}\text{B}_5\text{P}_4\text{Cl}_2\text{O}_1\text{Os}_1\text{Ru}_1$ , Calc. C, 59.68; H, 5.14%. Found: C, 59.55; H, 5.59%. LRMS: FAB (3-NBA and CsI). [ $\text{M} + \text{Cs}$ ] $^+$ : 1720.28, obs. 1720. The mass envelope for the observed spectrum for **5d** matches that calculated from known isotopic abundances of the constituent elements, as illustrated in Supp Table 4.

#### 2.5. Alternative preparation of $[2,2,2\text{-}(\text{PPh}_3)_2(\text{CO})\text{-nido-2-OsB}_4\text{H}_7\text{-3-(BH}_2\cdot\text{dppx}\cdot\text{Ru}(p\text{-cym})\text{Cl}_2)]$ (**5d**) from **1** and $[\text{dppx}\cdot\text{Ru}(p\text{-cym})\text{Cl}_2]$

A 50 mL round bottom flask was charged with 45 mg of  $[\text{dppx}\cdot\text{Ru}(p\text{-cym})\text{Cl}_2]$  (58 mmol) and 51 mg (1.1eq) of  $(\text{PPh}_3)_2(\text{CO})\text{OsB}_5\text{H}_9$ ; 15 mL of  $\text{CH}_2\text{Cl}_2$  was added and the mixture refluxed for 17 h. The solvent was then removed and the  $^{31}\text{P}$ ,  $^1\text{H}$  and  $^{11}\text{B}$  NMR spectrum of the crude product indicated the presence of **5d** along with decomposition products. Purification was effected using radial chromatography by dissolution of the product mixture in the minimum volume of  $\text{CH}_2\text{Cl}_2$  and application to a 1 mm plate where elution with  $\text{CH}_2\text{Cl}_2$  removed the non-ruthenium containing species. Addition of 10%  $\text{CH}_3\text{CN}$  to the  $\text{CH}_2\text{Cl}_2$  resulted in the formation a red band, and addition of a further 10%  $\text{CH}_3\text{CN}$  allowed isolation of a third band. The first and third bands consisted of **1** along with some impurities and a red non-boron containing substances, respectively. The second band afforded 49 mg (54% yield) of the red solid  $[2,2,2\text{-}(\text{PPh}_3)_2(\text{CO})\text{-nido-2-OsB}_4\text{H}_7\text{-3-(BH}_2\cdot\text{dppx}\cdot\text{Ru}(p\text{-cym})\text{Cl}_2)]$  (**5d**). Attempts to grow crystals suitable for X-ray diffraction proved unsuccessful but NMR spectra were identical to those described in the previous section.

#### 2.6. Preparation of $[2,2,2\text{-}(\text{PPh}_3)_2(\text{CO})\text{-nido-2-OsB}_4\text{H}_7\text{-3-(BH}_2\cdot\text{dppe}\cdot\text{Ru}(p\text{-cym})\text{I}_2)]$ (**6**)

In a process analogous to that for the preparation of **5b**, the product mixture from the reaction between 60 mg (0.075 mmol) of **1**, 62 mg (0.16 mmol) of dppe and 157 mg (0.16 mmol) of  $[\text{Ru}(p\text{-cym})\text{I}_2]_2$  in  $\text{CH}_2\text{Cl}_2$  was applied to the radial chromatograph using  $\text{CH}_2\text{Cl}_2$  as the mobile phase. Three bands were detected from this separation. The first band afforded a yellow solution which contained species **3**, **4**, and **1**, along with a trace amount of  $[2,2,2\text{-}(\text{PPh}_3)_2(\text{CO})\text{-nido-2-OsB}_4\text{H}_7\text{-3-(BH}_2\cdot\text{PPh}_3)]$ . The second band afforded a violet solution identified as  $[2,2,2\text{-}(\text{PPh}_3)_2(\text{CO})\text{-nido-2-OsB}_4\text{H}_7\text{-3-(BH}_2\cdot\text{dppe}\cdot\text{Ru}(p\text{-cym})\text{I}_2)]$  (**6**). The third band also gave a violet solution and this was shown by NMR

spectroscopy to consist of trace amounts of [dppe·(Ru(*p*-cym)I<sub>2</sub>)<sub>2</sub>] and [Ru(*p*-cym)I<sub>2</sub>]<sub>2</sub> starting material. From this separation 49 mg (39% yield, based on (PPh<sub>3</sub>)<sub>2</sub>(CO)OsB<sub>5</sub>H<sub>9</sub>), of **6** was obtained. Again attempts to grow crystals suitable from X-ray study were unsuccessful. <sup>1</sup>H NMR (CDCl<sub>3</sub>): *p*-cymene, (δ in ppm) 0.86 (d, *J* = 6.61 Hz, 3H, CHMe<sub>2</sub>), 0.85 (d, *J* = 6.49 Hz, 3H, CHMe<sub>2</sub>), 2.06 (s, 3H, Me), 3.08 (m, 1H, CHMe<sub>2</sub>), 4.85 (d, *J* = 5.81 Hz, 1H, MeC<sub>6</sub>H<sub>4</sub>CHMe<sub>2</sub>), 5.02 (d, *J* = 6.00 Hz, 1H, MeC<sub>6</sub>H<sub>4</sub>CHMe<sub>2</sub>), 5.15 (d, *J* = 5.91 Hz, 1H, MeC<sub>6</sub>H<sub>4</sub>CHMe<sub>2</sub>), 5.19 (d, *J* = 5.74 Hz, 1H, MeC<sub>6</sub>H<sub>4</sub>CHMe<sub>2</sub>); PPh<sub>2</sub>CH<sub>2</sub>CH<sub>2</sub>PPh<sub>2</sub>, (δ in ppm) 3.08 (m, 2H, CH<sub>2</sub>PPh<sub>2</sub>·Ru(*p*-cym)I<sub>2</sub>), 2.20 (m, 2H, BH<sub>2</sub>·PPh<sub>2</sub>CH<sub>2</sub>), 6.95–7.90 (m, 50H, Ph). The remaining <sup>1</sup>H data along with <sup>31</sup>P and <sup>11</sup>B can be found in Table 1. Elemental Anal.: **13a** for C<sub>73</sub>H<sub>77</sub>B<sub>5</sub>P<sub>4</sub>I<sub>2</sub>O<sub>1</sub>Os<sub>1</sub>Ru<sub>1</sub>, Calc. C, 51.78; H, 4.58. Found: C, 51.16; H, 5.10%. LRMS: Fab (3-NBA and CsI). Calc. for C<sub>73</sub>H<sub>78</sub>B<sub>5</sub>P<sub>4</sub>I<sub>2</sub>O<sub>1</sub>Os<sub>1</sub>Ru<sub>1</sub>[M + Cs + H]<sup>+</sup> 1828.39, obs 1828. The mass envelope for the observed spectrum of **6** matches that calculated from known isotopic abundances of the constituent elements and the data are given in Supplementary Table 5.

#### 2.7. Preparation of [BH<sub>3</sub>·(PPh<sub>2</sub>)(CH<sub>2</sub>)<sub>6</sub>(PPh<sub>2</sub>)·Ru(*p*-cym)Cl<sub>2</sub>] (7)

Dpph, 357 mg (0.47 mmol), was dissolved in 15 mL of freshly distilled CH<sub>2</sub>Cl<sub>2</sub> in a 50 mL round bottom flask containing a stir bar. A 10 mL solution of CH<sub>2</sub>Cl<sub>2</sub> containing 44 mg (0.072 mmol) [Ru(*p*-cym)Cl<sub>2</sub>]<sub>2</sub> was added and the mixture stirred at ambient temperature for 30 min. Passage through a 1 cm silica gel plug gave a colorless filtrate. CH<sub>3</sub>CN was then passed through the silica plug resulting in a deep red solution which was transferred to a 2-neck 50 mL flask and reduced to dryness on a rotary evaporator. The flask was then attached to the vacuum line, evacuated, and 20 mL of CH<sub>2</sub>Cl<sub>2</sub> condensed in at –196 °C. After warming to –78 °C, 1.3 mL of BH<sub>3</sub>·thf solution (1.3 mmol) was added under a dynamic flow of dry N<sub>2</sub>. The solution was stirred at this temperature for 15 min and then allowed to warm slowly to room temperature at which time it was exposed to air and passed through a 1 cm plug of silica giving a colorless filtrate. CH<sub>3</sub>CN was then poured through the silica plug forming a deep red colored solution which was then reduced to 1 mL in volume and applied to the radial chromatograph using CH<sub>2</sub>Cl<sub>2</sub> as the mobile phase. CH<sub>3</sub>CN was then slowly added to the eluent until a red band was detected. The red solution obtained from this band was evacuated to dryness affording 39 mg (69.9%) of a red solid which was characterized as [BH<sub>3</sub>·(PPh<sub>2</sub>)(CH<sub>2</sub>)<sub>6</sub>(PPh<sub>2</sub>)·Ru(*p*-cym)Cl<sub>2</sub>] (7). <sup>1</sup>H NMR (CDCl<sub>3</sub>): *p*-cymene, (δ in ppm) 0.89 (d, *J* = 6.96 Hz, 6H, CHMe<sub>2</sub>), 1.88 (s, 3H, Me), 2.52 (m, 1H, CHMe<sub>2</sub>), 5.08 (d, *J* = 6.00 Hz, 2H, MeC<sub>6</sub>H<sub>4</sub>CHMe<sub>2</sub>), 5.26 (d,

*J* = 6.60 Hz, 2H, MeC<sub>6</sub>H<sub>4</sub>CHMe<sub>2</sub>); PPh<sub>2</sub>(CH<sub>2</sub>)<sub>6</sub>PPh<sub>2</sub>, (δ in ppm) 2.05 (quart, *J* = 5.28 Hz, 2H, BH<sub>3</sub>·PPh<sub>2</sub>CH<sub>2</sub>), 1.56 (m, 2H, BH<sub>3</sub>·PPh<sub>2</sub>CH<sub>2</sub>CH<sub>2</sub>), 1.14 (m, 4H, BH<sub>3</sub>·PPh<sub>2</sub>CH<sub>2</sub>CH<sub>2</sub>CH<sub>2</sub>CH<sub>2</sub>), 0.99 (m, 2H CH<sub>2</sub>CH<sub>2</sub>·Ru(*p*-cym)Cl<sub>2</sub>), 2.52 (m, 2H, CH<sub>2</sub>PPh<sub>2</sub>·Ru(*p*-cym)Cl<sub>2</sub>), 7.39–7.81 (m, 20H, Ph); BH<sub>3</sub>, (δ in ppm) 0.89 (d, <sup>2</sup>*J*<sub>H-P</sub> = 16.09 Hz, 3H, BH<sub>3</sub>). <sup>31</sup>P{<sup>1</sup>H} NMR (CDCl<sub>3</sub>): (δ in ppm) 15.79 (*br*, BH<sub>3</sub>·PPh<sub>2</sub>CH<sub>2</sub>), 23.96 (s, CH<sub>2</sub>PPh<sub>2</sub>·Ru(*p*-cym)Cl<sub>2</sub>). <sup>11</sup>B{<sup>1</sup>H} NMR (CDCl<sub>3</sub>): (δ in ppm) –39.42 (s, BH<sub>3</sub>). HRMS: Calc. for <sup>12</sup>C<sub>40</sub><sup>1</sup>H<sub>49</sub><sup>31</sup>P<sub>2</sub><sup>35</sup>Cl<sub>1</sub><sup>11</sup>B<sub>1</sub><sup>102</sup>Ru<sub>1</sub> [M – Cl]<sup>+</sup> 739.2135, obs. 739.2160, standard deviation 3.4 ppm.

#### 2.8. X-ray structure determination of [BH<sub>3</sub>·(PPh<sub>2</sub>)(CH<sub>2</sub>)<sub>6</sub>(PPh<sub>2</sub>)·Ru(*p*-cym)Cl<sub>2</sub>] (7)

Red irregular crystals of **7** were formed from a CH<sub>2</sub>Cl<sub>2</sub>/Et<sub>2</sub>O solution at 5 °C. A crystal with dimensions 0.38 × 0.33 × 0.20 mm<sup>3</sup> was mounted on a glass fiber in a random orientation. Preliminary examination and data collection was performed using a Bruker SMART Charge Coupled Device (CCD), detector system, single crystal X-ray diffractometer using graphite monochromated Mo Kα radiation (λ = 0.71073) equipped with a sealed tube X-ray source at –60 °C. Preliminary unit cell constants were determined with a set of 45 narrow frames (0.3° in ω) scans. The data set collected consists of 4028 frames of intensity data collected with a frame width of 0.3° in ω and counting time of 30 s/frame at a crystal to detector distance of 4.930 cm. The double pass method of scanning was used to exclude any noise. The collected frames were integrated using an orientation matrix determined from the narrow frame scans. SMART and SAINT software packages [12] were used for data collection and data integration. Analysis of the integrated data did not show any decay. Final cell constants were determined by a global refinement of *xyz* centroids of 61 725 reflections (5° < 2θ < 56°). Collected data were corrected for systematic errors using SADABS [13] based on the Laue symmetry using equivalent reflections. The integration process yielded 46346 reflections of which 9059 were independent.

Crystal data and intensity data collection parameters are listed in Table 2. Structure solution and refinement were carried out using the SHELXTL-PLUS [14] software package. The structure was solved by the Patterson method and refined successfully in the space group *P* $\bar{1}$ . Full matrix least-squares refinement was carried out by minimizing  $\sum w(F_o^2 - F_c^2)^2$ . The non-hydrogen atoms were refined anisotropically to convergence. All cage hydrogen atoms were located and refined freely. The other hydrogen atoms were treated using an appropriate riding model (AFIX m3). A projection view of the molecule with non-hydrogen atoms represented by 50%

probability ellipsoids, and showing the atom labeling is presented in Fig. 2.

Selected bond lengths and angles are given in Table 3, and a complete list of bond length and angles as well as listings of positional and isotropic displacement coefficients for hydrogen atoms, anisotropic displacement coefficients for the non-hydrogen atoms can be found in the supplementary material.

### 3. Results

The reaction between the *nido*-*o*-hexaborane,  $(\text{PPh}_3)_2(\text{CO})\text{OsB}_5\text{H}_9$  (**1**), and bidentate phosphines of the type  $\text{PPh}_2\text{C}_x\text{H}_y\text{PPh}_2$ , affords species **2** as illustrated in Scheme 1. If a solution of  $[2,2,2-(\text{PPh}_3)_2(\text{CO})\text{-nido-2-OsB}_4\text{H}_7\text{-3-(BH}_2\cdot\text{PPh}_2\text{C}_x\text{H}_y\text{PPh}_2)]$  (**2a**, **2b**, **2c**) [1a], is allowed to stand rearrangement to species **4**, also shown in Scheme 1, proceeds. In this process the distal end of the  $\text{BH}_2\cdot\text{PPh}_2\text{C}_x\text{H}_y\text{PPh}_2$  moiety, an uncoordinated phosphine, displaces a phosphine ligand on the Os atom to afford  $[\{(\text{PPh}_3)(\text{CO})\text{OsB}_4\text{H}_7\}\text{-}\eta^2\text{-3,2-\{BH}_2\cdot\text{PPh}_2\text{C}_x\text{H}_y\text{PPh}_2\}]$  (**4**). The basicity of the pendent phosphine in species of type **2** was demonstrated by the reaction of  $[2,2,2-(\text{PPh}_3)_2(\text{CO})\text{-nido-2-OsB}_4\text{H}_7\text{-3-(BH}_2\cdot\text{PPh}_2\text{C}_3\text{H}_6\text{PPh}_2)]$  (**2b**) with  $\text{BH}_3\cdot\text{thf}$  to afford  $[2,2,2-(\text{PPh}_3)_2(\text{CO})\text{-nido-2-OsB}_4\text{H}_7\text{-3-(BH}_2\cdot\text{PPh}_2\text{C}_3\text{H}_6\text{PPh}_2\cdot\text{BH}_3)]$  [1a]. To probe the reactivity of this uncoordinated phosphine further in species **2a–2c**, it was allowed to react with the species  $[\text{Ru}(p\text{-cym})\text{Cl}_2]_2$ . The dimer of the 16-electron ruthenium species is cleaved by phosphines to produce a monomeric species of the type  $\text{PR}_3\cdot\text{Ru}(p\text{-cym})\text{Cl}_2$  [15]. The  $(\eta^6\text{-}p\text{-cym})$ ruthenium(II) complex was selected because it has been used as a vertex in metallaboranes [16] and there are characteristic  $^1\text{H}$  NMR signals for the *p*-cymene group. The latter acts as a good indicator that the final product contains the  $\text{Ru}(p\text{-cym})\text{Cl}_2$  fragment. Further, the chloride present on the ruthenium center can be replaced by larger halide or halide analogue [9] and thereby provide information on the role the halide has on the system.

Stirring a mixture of **1** and excess  $[(\text{PPh}_2)_2(\text{CH}_2)_3](\text{dppe})$  in  $\text{CH}_2\text{Cl}_2$  for 12 hours followed by addition of a small excess of  $[\text{Ru}(p\text{-cym})\text{Cl}_2]_2$  affords a red solid in which the distal end of the  $\text{BH}_2\cdot\text{PPh}_2\text{C}_2\text{H}_4\text{PPh}_2$  moiety has been functionalized to form  $[2,2,2-(\text{PPh}_3)_2(\text{CO})\text{-nido-2-OsB}_4\text{H}_7\text{-3-(BH}_2\cdot\text{PPh}_2\text{C}_2\text{H}_4\text{PPh}_2\cdot\text{Ru}(p\text{-cym})\text{Cl}_2)]$  (**5a**). The overall yield of this reaction is relatively low (33% yield based on **1**), presumably due to the competing intramolecular reaction **2a** undergoes to produce **4a**. In an effort to preclude this, a different synthetic route was utilized in which one end of the bidentate phosphine was already attached to the  $\text{Ru}(p\text{-cym})\text{Cl}_2$  fragment prior to reaction with **1**. A typical process, utilizing the two approaches, is illustrated in Scheme 2. Surprisingly, this did not increase the yield by more than 25%

Table 2  
Crystal data and structure refinement for **7**

Empirical formula	$\text{C}_{40}\text{H}_{49}\text{BCl}_2\text{P}_2\text{Ru}$
Formula weight	774.51
Temperature (K)	223(2)
Wavelength (Å)	0.71073
Crystal system	triclinic
Space group	$\bar{P}1$
<i>Unit cell dimensions</i>	
<i>a</i> (Å)	10.0759(1)
<i>b</i> (Å)	12.1798(1)
<i>c</i> (Å)	16.0963(1)
$\alpha$ (°)	90.109(1)
$\beta$ (°)	93.07(1)
$\gamma$ (°)	106.427(1)
Volume (Å <sup>3</sup> )	1891.72(3)
<i>Z</i>	2
Density (calculated) (Mg/m <sup>3</sup> )	1.360
Absorption coefficient (mm <sup>-1</sup> )	0.667
<i>F</i> (000)	804
Crystal size (mm <sup>3</sup> )	$0.38 \times 0.33 \times 0.20$
$\theta$ Range for data collection	1.74–28.00.
Index ranges	$-13 \leq h \leq 13, -16 \leq k \leq 16, -21 \leq l \leq 21$
Reflections collected	46346
Independent reflections [ <i>R</i> <sub>int</sub> ]	9059 [0.04]
Completeness to $\theta = 28.00^\circ$	99.0%
Absorption correction	empirical
Maximum and minimum transmission	0.8781 and 0.7855
Refinement method	full-matrix least-squares on <i>F</i> <sup>2</sup>
Data/restraints/parameters	9059/3/430
Goodness-of-fit on <i>F</i> <sup>2</sup>	1.043
Final <i>R</i> indices [ <i>I</i> > 2σ( <i>I</i> )]	<i>R</i> <sub>1</sub> = 0.0270, <i>wR</i> <sub>2</sub> = 0.0617
<i>R</i> indices (all data)	<i>R</i> <sub>1</sub> = 0.0358, <i>wR</i> <sub>2</sub> = 0.0658
Largest differential peak and hole (e Å <sup>-3</sup> )	0.435 and -0.435

and thus only one of these experiments is included in this report. Reasons for the low yields include degradation of the metal-containing species on the silica surface during purification by thin layer chromatography or incomplete removal of product from the silica surface. NMR experiments on the crude reaction mixture indicated that there was essentially quantitative conversion of **2a** to **5a**. The proposed structure of  $[2,2,2-(\text{PPh}_3)_2(\text{CO})\text{-nido-2-OsB}_4\text{H}_7\text{-3-(BH}_2\cdot\text{PPh}_2\text{C}_2\text{H}_4\text{PPh}_2\cdot\text{Ru}(p\text{-cym})\text{Cl}_2)]$  (**5a**) given in Fig. 1 conforms to the elemental analytical and mass spectral data presented

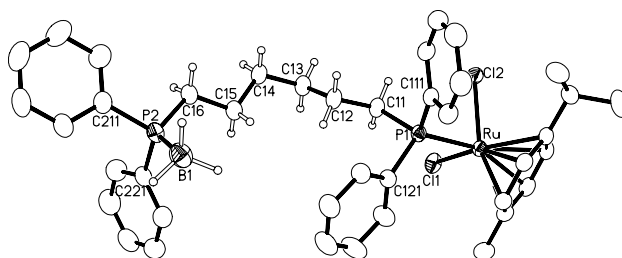
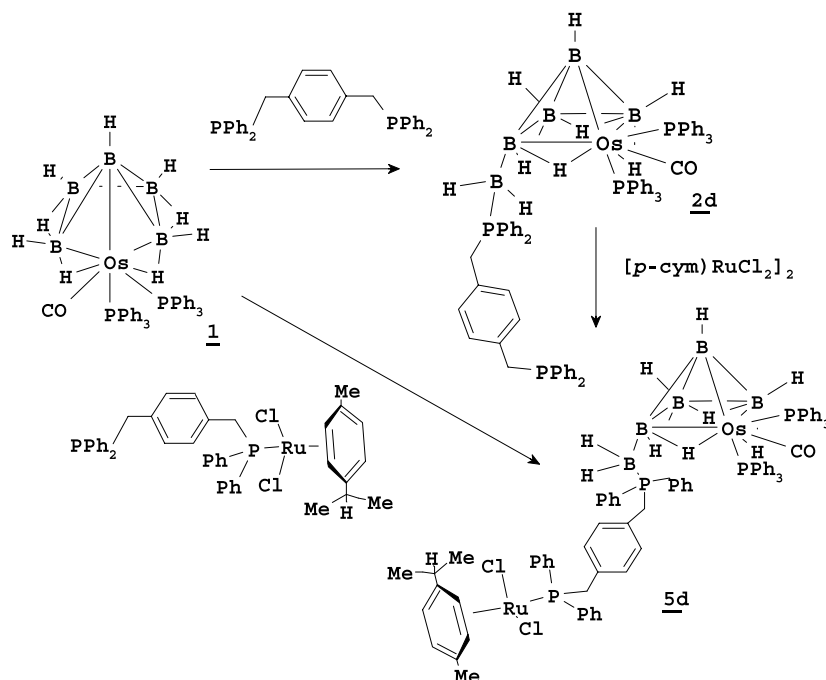


Fig. 2. Structure of  $[\text{BH}_3\cdot(\text{PPh}_2)(\text{CH}_2)_6(\text{PPh}_2)\cdot\text{Ru}(p\text{-cym})\text{Cl}_2]$  (**7**) with ellipsoids drawn at the 50% probability level. H atoms on phenyl rings and their substituents are omitted for clarity.



Scheme 2.

herein although crystals suitable for X-ray analysis were not available.

The  $^{31}\text{P}\{^1\text{H}\}$  NMR spectrum of **5a** at 298 K exhibited three resonances in 2:1:1 area ratio. A broad one assigned to overlapping dppe signals (+22.28 ppm), and two signals from the PPh<sub>3</sub> groups coordinated to the Os center. When cooled to 260 K the signal assigned to the dppe ligand could be resolved into two doublets at +22.21 ( $J = 35.19$  Hz) and +23.15 ( $J = 36.87$  Hz) ppm which 2D  $^1\text{H}$ - $^{31}\text{P}$ -COSY experiments allowed assignment as the phosphorus atom bound to the BH<sub>2</sub> moiety and that bound to the ruthenium center, respectively. The  $^{11}\text{B}$  NMR spectrum of **5a** gave the expected 4 peaks in 2:1:1:1 area ratio confirming the presence of five boron atoms. The data are found in Table 1 and correspond well to those for the other osmahexaboranes to which a phosphine is coordinated [1,2a]. Of note is the resonance at -38.03 ppm arising from the BH<sub>2</sub> moiety directly bound to a phosphorus atom of the dppe ligand; in the expected range for phosphine-borane moieties [17]. The  $^1\text{H}\{^{11}\text{B}\}$  spectrum of **5a** afforded the expected nine resonances of area ratio one assigned to five terminal and four bridging hydrogen atoms. At room temperature two complex multiplets at +2.85 and +2.34 ppm were observed for the methylene protons on the dppe backbone. At 260 K three resonances were observed for these methylene protons in a 1:1:2 area ratio. The first two, at +2.80 and +2.73 ppm, both complex multiplets, were assigned to the methylene protons adjacent to the PPh<sub>2</sub>·Ru(*p*-cym)Cl<sub>2</sub> fragment and the resonance of area ratio two, at +2.29 ppm, was assigned

to the methylene protons adjacent to the BH<sub>2</sub>·PPh<sub>2</sub> group.

The resonances for the *p*-cymene ligand were quite interesting and somewhat unexpected and they differed at 298 and 260 K. A schematic representation of the *p*-cymene ligand along with a numbering scheme is shown in Fig. 3. At room temperature two sets of doublets at +0.96 and +0.93 ppm assigned to the two-methyl groups occupying positions 1 and 1' were observed, but at 260 K these signals coalesce to a complex multiplet. The methyne proton at position 2 is observed as the expected septet and the methyl group at position 5 is observed as a singlet at both temperatures. At room temperature an apparent triplet and two doublets in a 2:1:1 ratio are observed for the aromatic protons, assigned to the protons occupying positions 4 and

Table 3  
Selected bond distances (Å) and angles (°) for (7)

Ru-P(1)	2.3626(4)	Ru-Cl(1)	2.4270(5)
Ru-Cl(2)	2.4020(4)	P(1)-C(111)	1.8198(19)
P(1)-C(121)	1.8307(18)	P(1)-C(11)	1.8363(18)
P(2)-B(1)	1.923(3)	P(2)-C(211)	1.818(2)
P(2)-C(16)	1.8233(19)	P(2)-C(221)	1.815(2)
C(11)-C(12)	1.521(2)	C(15)-C(16)	1.526(3)
P(1)-Ru-Cl(1)	88.074(16)	P(1)-Ru-Cl(2)	82.895(15)
Cl(1)-Ru-Cl(2)	89.568(17)	C(111)-P(1)-C(121)	103.86(8)
C(111)-P(1)-C(11)	106.68(8)	C(121)-P(1)-C(11)	100.78(8)
C(111)-P(1)-Ru	111.76(5)	C(121)-P(1)-Ru	118.98(6)
C(11)-P(1)-Ru	113.46(6)	C(221)-P(2)-C(211)	106.12(9)
C(221)-P(2)-C(16)	106.45(9)	C(211)-P(2)-C(16)	103.59(9)
C(211)-P(2)-B(1)	111.34(11)	C(12)-P(2)-B(1)	112.21(11)
C(16)-P(2)-B(1)	116.34(11)	C(12)-C(11)-P(1)	120.73(14)
C(15)-C(16)-P(2)	115.69(14)	C(12)-C(13)-C(14)	113.93(16)

4' overlapping, and at 3 and 3', respectively. At 260 K the triplet resolves into two doublets, each of area ratio one; the higher field pair assigned to 4 and 4', and the lower field pair to 3 and 3'; all assignments made on the basis of 2D HH-COSY and HH-ROESY experiments. The NMR data, all of which conform to the structure given in Fig. 1 are listed in Table 1.

Similar results were obtained when using the phosphines [(PPh<sub>2</sub>)<sub>2</sub>(CH<sub>2</sub>)<sub>3</sub>] (dppp) and [(PPh<sub>2</sub>)<sub>2</sub>(CH<sub>2</sub>)<sub>6</sub>] (dpph), resulting in the formation of **5b** and **5c**, respectively. Mass spectral data were obtained for both and although the elemental analysis for **5b** were not as good as those for **5a** and **5c**, the data obtained from NMR spectroscopy, shown in Table 1, along with mass spectral data confirmed the formulation of **5b**.

Since the NMR spectra for the *p*-cymene ligands in **5a**, **5b** and **5c** were similar in spite of varying the length of the alkyl bridge in the bidentate phosphines, we chose to use the rigid backbone species dppx. Reactions of **1** with phosphines with rigid backbones such as PPh<sub>2</sub>XPPH<sub>2</sub> {X = 1,4-C<sub>6</sub>H<sub>4</sub> (arphos)}, 1,4-CH<sub>2</sub>C<sub>6</sub>H<sub>4</sub>CH<sub>2</sub> (dppx), and Fe(C<sub>5</sub>H<sub>4</sub>)<sub>2</sub> (dppf) had previously been examined in our laboratory [1c]. In a typical reaction, dppx was allowed to react with **1** to produce the species [2,2,2-(PPh<sub>3</sub>)<sub>2</sub>(CO)-*nido*-2-OsB<sub>4</sub>H<sub>7</sub>-3-(BH<sub>2</sub>·PPh<sub>2</sub>CH<sub>2</sub>C<sub>6</sub>H<sub>4</sub>CH<sub>2</sub>PPH<sub>2</sub>)] (**2d**), which was then treated with [Ru(*p*-cym)Cl<sub>2</sub>]<sub>2</sub> to form the red solid [2,2,2-(PPh<sub>3</sub>)<sub>2</sub>(CO)-*nido*-2-OsB<sub>4</sub>H<sub>7</sub>-3-(BH<sub>2</sub>·PPh<sub>2</sub>CH<sub>2</sub>C<sub>6</sub>H<sub>4</sub>CH<sub>2</sub>PPH<sub>2</sub>·Ru(*p*-cym)Cl<sub>2</sub>)] (**5d**). The isolated yield of **5d** obtained (46%) was higher than that for its precursor **2d**, presumably because in solution **2d** can react further to form the linked cluster system [{2,2,2-(PPh<sub>3</sub>)<sub>2</sub>(CO)-*nido*-2-OsB<sub>4</sub>H<sub>7</sub>}]<sub>2</sub> (dppx) [1c], however coordination to the metal center in **5d** this precludes this formation. It was also found by monitoring the <sup>31</sup>P{<sup>1</sup>H} NMR spectrum over time that the stability of **5d** in solution was higher than that of its precursor **2d**.

Species **5a–d** were also prepared by the reaction between **1** and the bidentate phosphine to which a [(*p*-cym)RuCl<sub>2</sub>] moiety was coordinated to one end. We only describe that for **5d**, which was formed in 54% yield from **1** and [dppx·Ru(*p*-cym)Cl<sub>2</sub>] (Scheme 2). Spectral data for the cage and the *p*-cym moiety in **5d** were similar to those for **5a–c**, and are given in Table 1. Similarly, the spectra for the hydrocarbon linker in **5d** are not unusual and are given in the experimental section. The <sup>31</sup>P resonance for the dppx P atom bonded to the Ru center is observed as a doublet, due to coupling to the other P

center, which is inequivalent. Such coupling is observed for **5a–c** but in this case it represents a 7-bond interaction between the two dppx ligand P atoms (<sup>7</sup>J<sub>P–P</sub> = 4.88 Hz). Coupling of this type has been observed before in similar systems and confirmed by 2D[<sup>31</sup>P–<sup>31</sup>P]-COSY experiments [1,18].

Since changing the nature of the bidentate phosphines used did not affect the NMR spectroscopic properties of the hybrid system, the next step was to change the halide present on the ruthenium fragment. Thus we replaced the chloride by iodide in the starting [Ru(*p*-cym)Cl<sub>2</sub>]<sub>2</sub> complex [9] to see if the halide played a role in these systems. The reaction conditions used were similar to those in which **5a** was isolated. Briefly dppe was allowed to react with **1** to form [2,2,2-(PPh<sub>3</sub>)<sub>2</sub>(CO)-*nido*-2-OsB<sub>4</sub>H<sub>7</sub>-3-(BH<sub>2</sub>·PPh<sub>2</sub>C<sub>2</sub>H<sub>4</sub>PPH<sub>2</sub>)] (**2a**), and to this a slight excess of [Ru(*p*-cym)I<sub>2</sub>]<sub>2</sub> added. From this reaction mixture a deep red solid, identified as [2,2,2-(PPh<sub>3</sub>)<sub>2</sub>(CO)-*nido*-2-OsB<sub>4</sub>H<sub>7</sub>-3-(BH<sub>2</sub>·PPh<sub>2</sub>C<sub>2</sub>H<sub>4</sub>PPh<sub>2</sub>·Ru(*p*-cym)I<sub>2</sub>)] (**6**) was isolated in 39% yield. The overall yield is comparable to that obtained for **5a** (33%) and we ascribe the slight increase to the ease in which **2d** was removed from the silica surface since CH<sub>3</sub>CN was not required to aid removal from the surface of the silica, as it was for the isolation of **5a**. Spectral data for **6** were quite similar to those for **5a–d**, with some subtle differences. The dppe <sup>31</sup>P resonances for **5a** were broad at 298 K but sharpened at 260 K to two doublets, however the spectrum for **6** at 298 K resembled that for **5a** at 260 K and did not change appreciably on cooling.

As part of this overall study, we prepared a series of bidentate phosphines which had organotransition metal and borane moieties at each end. This work will be described in detail in the next paper in this series, but herein we describe the structure of the species [BH<sub>3</sub>·(PPh<sub>2</sub>)(CH<sub>2</sub>)<sub>6</sub>(PPh<sub>2</sub>)·Ru(*p*-cym)Cl<sub>2</sub>] (**7**). At –78 °C and under a flow of N<sub>2</sub>, BH<sub>3</sub>·thf was introduced into a CH<sub>2</sub>Cl<sub>2</sub> solution of [C<sub>6</sub>H<sub>12</sub>PPh<sub>2</sub>·Ru(*p*-cym)Cl<sub>2</sub>], prepared *in situ* from dpph and [Ru(*p*-cym)Cl<sub>2</sub>]<sub>2</sub>. Essentially a quantitative yield of **7** was obtained as a red solid, although due to adherence of **7** to the silica gel during purification, the isolated yield was 70%. Two peaks of equal area were observed in the <sup>31</sup>P{<sup>1</sup>H} NMR spectrum of **7**, the sharper of the two, falling at +23.96 ppm, was assigned to the phosphine directly bound to the ruthenium moiety. The second quite broad peak, observed at +15.79 ppm was assigned to the phosphine bonded to the BH<sub>3</sub> fragment. Coupling between the two P atoms was not observed. The <sup>11</sup>B{<sup>1</sup>H} spectrum of **7** contained a single resonance at –39.42 ppm, typical for a phosphine–borane moiety [6–8]. The <sup>1</sup>H{<sup>11</sup>B} NMR spectrum of **7** is given in the experimental section and all the protons were fully identified. Of note is the fact that for the *p*-cym ligand, a single doublet is observed at +0.89 ppm, assigned to the methyl groups at positions

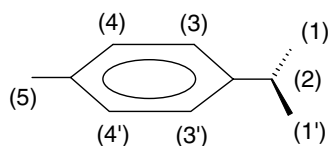


Fig. 3. A schematic representation of the *p*-cymene ligand showing the numbering scheme.

1 and 1' and single doublets were observed for each of the pairs of aromatic protons, 3/3' and 4/4'. All other protons were assigned and all assignment made on the basis of 2D NMR experiments carried out at 303 K.

Red irregular crystals of **7** suitable for X-ray analysis were formed from a CH<sub>2</sub>Cl<sub>2</sub>/Et<sub>2</sub>O solution at 5 °C. The structure resembles that expected for **5a** except that the (PPh<sub>3</sub>)<sub>2</sub>(CO)OsB<sub>4</sub>H<sub>7</sub>-BH<sub>2</sub> moiety has been replaced by a BH<sub>3</sub> group. There are no unexpected features associated with the structure of **7**. The environment around P(1), which is coordinated to the Ru moiety, deviates from ideal tetrahedral geometry to a greater degree than that around P(2). For P(1) the angles range from ca. 100.78–118.98°, and for P(2) the angles range from ca. 103.59–116.34°. The angles around P(1) deviate further from an ideal tetrahedral geometry than they do around P(2) because the Ru moiety is much more sterically encumbering than the BH<sub>3</sub> moiety coordinated to P(2). Small differences can also be seen for the P–C(alkyl) bond lengths. Thus P(1)–C(11) has a bond length of 1.836(2) Å, while for P(2)–C(16) a bond length of 1.823(2) Å is observed and this, perhaps may be ascribed to P(1) donating more electron density to ruthenium than P(2) donates to boron.

#### 4. Discussion

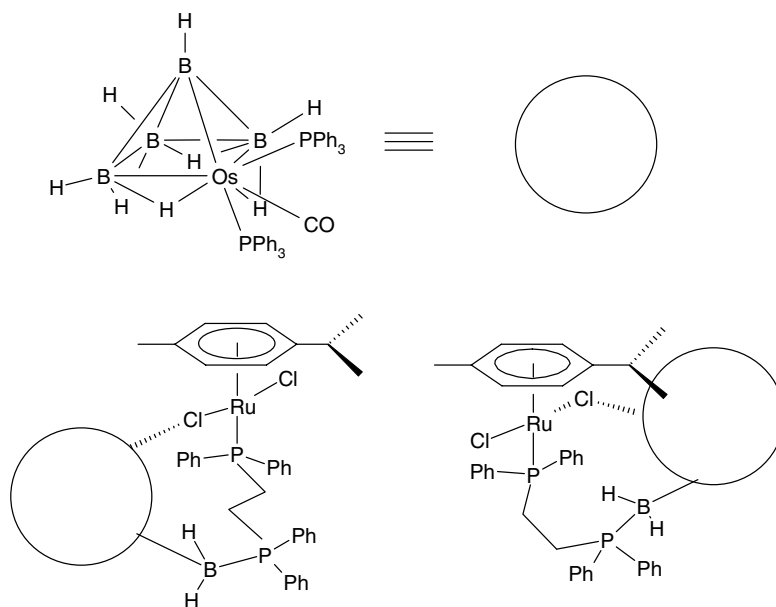
This study has demonstrated that species of the type [ {(PPh<sub>3</sub>)<sub>2</sub>(CO)OsB<sub>4</sub>H<sub>7</sub> }-3- {BH<sub>2</sub>PPh<sub>2</sub>(CH<sub>2</sub>)<sub>n</sub>(PPh<sub>2</sub>) } ] (**2**) can be used as substrates for the formation of hybrid systems of the type [ 2,2,2-(PPh<sub>3</sub>)<sub>2</sub>(CO)-*nido*-2-OsB<sub>4</sub>H<sub>7</sub>-3-(BH<sub>2</sub>PPh<sub>2</sub>)C<sub>x</sub>H<sub>y</sub>PPh<sub>2</sub>RuCl<sub>2</sub>(*p*-cym) ]. (**5**) This is in spite of the tendency for **2** to undergo intramolecular substitution reactions. This latter behavior precluded isolation of crystals suitable for X-ray analysis however NMR spectra, high resolution mass spectrometry and elemental analysis confirmed the structures. Furthermore, a crystal structure determination of the closely related species [BH<sub>3</sub>·(PPh<sub>2</sub>)(CH<sub>2</sub>)<sub>6</sub>(PPh<sub>2</sub>)·Ru(*p*-cym)Cl<sub>2</sub>] (**7**), along with detailed NMR studies supports our conclusions about the identity of **5a–d** and **6**.

Perhaps the most unusual observation was the proton NMR data for the *p*-cym ligands in **5a–d** and **6**. Since the *p*-cym moiety has a plane of symmetry, it was expected that only 5 resonances would be observed, a singlet for the unique methyl group, a septet for the *i*-propyl proton, a doublet for the methyl groups of the *i*-propyl moiety and two doublets in an AB pattern for the aromatic protons. This however was not the case since in addition to the septet and the singlet, two resonances for each of the methyl groups at positions 1, 1' (see Fig. 3), and two sets of doublets for each of the two pairs of equivalent aromatic protons at positions 3,3' and 4,4' were observed. Altering the chain length of the bidentate

phosphine, changing the nature of the chain and also the halogen bonded to the Ru atom did not alter this observation. The only changes we did observe was that for **5d**, <sup>31</sup>P–<sup>31</sup>P coupling was observed between the two dppx P atoms; seven bond coupling presumably facilitated by delocalization through the π-cloud of the arene ring, and the effect on the line widths of the resonances for P(3) and P(4) in **6**. The effects on the *p*-cym ligand were more profound for **5a** than for **5b** or **5c**, suggesting that the proximity of the *nido*-osmaborane cluster increases this influence. Attempts to prepare the dppm ([ (PPh<sub>2</sub>)<sub>2</sub>CH<sub>2</sub> ]) analogue of **5a–d** were unsuccessful, so observation of the effect of shortening the length of the alkyl backbone was not possible.

The NMR data obtained for **5a–d** and **6** indicated that only a single species was present in solution and 2D NMR experiments suggested that there were neither anomalous couplings nor short range through-space interactions to account for the observed doubling pattern. The only remaining feature that could have caused these doublings was the *nido*-osmapentaborane cluster tethered at the distal end of the PPh<sub>2</sub>C<sub>x</sub>H<sub>y</sub>PPh<sub>2</sub>·Ru(*p*-cym)Cl<sub>2</sub> moiety. This hypothesis is further enhanced since this anomalous phenomenon was not observed for **7** which contains a BH<sub>3</sub> group rather than the *nido*-osmapentaborane moiety [ (PPh<sub>3</sub>)<sub>2</sub>(CO)OsB<sub>4</sub>H<sub>7</sub> (BH<sub>2</sub>) ].

The type of behavior observed for the *p*-cymene ligand and has been previously reported in the literature in cases where there is asymmetry at the metal center [19]. The only asymmetric feature in the series of species **5a–d** and **6** resides in the osmaborane cluster. The appended BH<sub>2</sub> at position 3 on the osmaborane cluster in species of type **2** and those containing monodentate phosphines [1a] exhibit two inequivalent terminal proton resonances for **6** and **6'** (see Table 1 and Fig. 1), which feature symmetrical, mirror-image fine structure which we attribute to long range <sup>1</sup>H and <sup>31</sup>P coupling and which results in an apparent doublet structure. This is consistent with the structure because the two hydrogens are on a prochiral center and are, therefore, diastereotopic thus exhibiting different chemical shifts and splitting each other. Technically the *nido*-osmapentaborane cluster renders the protons on the *p*-cymene ligand diastereotopic, but in some cases the chiral cluster is eleven bonds removed from the *p*-cymene ligand and thus the effect would be expected to be minimal. This is not the case however, as experimental observations portend to the contrary. We mentioned earlier that the NMR spectra obtained for **6** at 298 K were similar to those obtained for **5a** at 260 K. This suggested that the halide present at the ruthenium center does play some role in the diastereotopic behavior observed at the *p*-cymene ligand. One possible explanation for this is that in solution the *nido*-osmapentaborane cluster is associating, via

Fig. 4. Possible solution configurations of **5**.

hydrogen bonding, to the halide at the ruthenium center. Thus the *nido*-osmapentaborane cluster finds itself in closer proximity to the ruthenium center, magnifying the effect of this chiral unit on the *p*-cymene ligand. Examples of conformations that could arise from this interaction are shown in Fig. 4. The cartoon type depiction given shows two possible conformations that could exist in solution for species **5a** and this could be extended to include the other species in the series. Unfortunately we could not obtain further corroborating evidence such as crystal structure data that would confirm this hypothesis. If this explanation is correct, it would represent one of the first reported examples of a chiral unit causing a diastereotopic effect on a ligand that is up to eleven bonds removed from the chiral moiety.

### Acknowledgements

We acknowledge the NSF (Grant No. CHE-9727570), the Missouri Research Board and UM-St. Louis for research grants to LB, and the NSF, the UM-St. Louis Center for Molecular Electronics and the Missouri Research Board for funds that helped purchase the XRD, NMR, and MS facilities. We also thank Mr. Joe Kramer for help with the MS measurements.

### Appendix A. Supplementary data

Supplementary data associated with this article can be found, in the online version at [doi:10.1016/j.ica.2004.10.015](https://doi.org/10.1016/j.ica.2004.10.015).

### References

- [1] (a) P. McQuade, K. Hupp, J. Bould, H. Fang, N.P. Rath, R.L. Thomas, L. Barton, *Inorg. Chem.* 38 (1999) 5415; (b) P. McQuade, in: M.G. Davidson, A.K. Hughes, T.B. Marder, K. Wade (Eds.), *Contemporary Boron Chemistry*, Special Publication, vol. 253, Royal Society of Chemistry, 2000, pp. 271–275; (c) P. McQuade, R.E.K. Winter, L. Barton, *J. Organomet. Chem.* 688 (2003) 82.
- [2] (a) L. Barton, J. Bould, H. Fang, K. Hupp, N.P. Rath, C. Gloeckner, *J. Am. Chem. Soc.* 119 (1997) 631; (b) X. Lei, M. Shang, T.P. Fehlner, *Organometallics* 19 (2000) 5266; (c) L.N. Pangan, Y. Kawano, M. Shimoi, *Organometallics* 19 (2000) 5575; (d) Y. Kawano, K. Kawakami, M. Shimoi, *Chem. Lett.* (2001) 1006; (e) L.N. Pangan, Y. Kawano, M. Shimoi, *Inorg. Chem.* 40 (2001) 1985; (f) R. Macias, T.P. Fehlner, A.M. Beatty, *Angew. Chem., Int. Ed.* 41 (2002) 3860; (g) R. Macias, T.P. Fehlner, A.M. Beatty, *Organometallics* 23 (2004) 2124.
- [3] (a) R.E. Williams, *Adv. Inorg. Chem. Radiochem.* 18 (1976) 67; (b) K. Wade, *Adv. Inorg. Chem. Radiochem.* 18 (1976) 60; (c) R.W. Rudolph, *Acc. Chem. Res.* 9 (1976) 446.
- [4] D.F. Shriver, M.A. Drezdon, *The Manipulation of Air-Sensitive Compounds*, John Wiley, New York, 1986.
- [5] J. Bould, M.N. Greenwood, J.D. Kennedy, *J. Organomet. Chem.* 249 (1983) 11.
- [6] D. Imhof, U. Burckhardt, K.-H. Dahmen, F. Joho, R. Nesper, *Inorg. Chem.* 36 (1997) 1813.
- [7] P. McQuade, N.P. Rath, L. Barton, *Inorg. Chem.* 38 (1999) 5468.
- [8] M.A. Bennett, T.-N. Huang, T.W. Matteson, A.K. Smith, *Inorg. Synth.* 21 (1982) 74.
- [9] R.A. Zelonka, M.C. Baird, *Can. J. Chem.* 50 (1972) 3063.
- [10] Assignments of the NMR spectra listed in Table 1, were based on detailed analyses previously reported in [1a,1c,5], and on spectra and X-ray structural data for [2,2,2-(PPh<sub>3</sub>)<sub>2</sub>(CO)-*nido*-2-OsB<sub>4</sub>H<sub>7</sub>-3-(BH<sub>2</sub>PPh<sub>2</sub>Me)] [2a] and for [2,2,2-(PPh<sub>3</sub>)<sub>2</sub>(CO)-*nido*-2-OsB<sub>5</sub>H<sub>9</sub>]

- found in 5 and in J. Bould, J.D. Kennedy, R.L.I. Thomas, L. Barton, N.P. Rath, *Acta Crystallogr. Sect. C* 57 (2001) 1245.
- [11] We found that the use of CsI in FAB Mass Spectrometry substantially simplified the spectra by avoiding overlap of peak envelopes. See G. Siuzdak, S.V. Wendeborn, K.C. Nicolaou, *Int. J. Mass Spectrom. Ion Proc.* 112 (1992) 79.
- [12] Bruker Analytical X-ray Division, Madison, WI, 1998.
- [13] R.H. Blessing, *Acta Crystallogr. Sect. A* 51 (1995) 33.
- [14] G.M. Sheldrick, Bruker Analytical X-ray Division, Madison, WI, 1999.
- [15] S.A. Serron, S.P. Nolan, Yu.A. Abramov, L. Brammer, J.L. Petersen, *Organometallics* 17 (1998) 104.
- [16] (a) See for example: M. Bown, X.L.R. Fontaine, N.N. Greenwood, J.D. Kennedy, M. Thornton-Pett, *Organometallics* 6 (1987) 2254;  
(b) J.H. Davis, E. Sinn, R.N. Grimes, *J. Am. Chem. Soc.* 111 (1989) 4776;  
(c) R.L.I. Thomas, A. J.J. Chem. Soc. Dalton Trans. (1997) 631;  
(d) R.L.I. Thomas, L. Barton, *Inorg. Chim. Acta* 289 (1999) 134.
- [17] (a) H. Nöth, B. Wrackmeyer, *Nuclear Magnetic Resonance Spectroscopy of Boron Compounds*, Springer Verlag, Heidelberg, 1978, pp. 340–344;  
(b) K.C. Nainan, G.E. Ryschewitsch, *Inorg. Chem.* 8 (1969) 2671.
- [18] (a) K. Gholivand, A.H. Mahmoudkhani, M. Khosravi, *Phosphorus, Sulfur Silicon Relat. Elem.* 106 (1995) 173;  
(b) R. Macias, N.P. Rath, L. Barton, *J. Chem. Soc., Chem. Commun.* (1998) 1091.
- [19] (a) For example see: N. Nul, J.H. Nelson, *Organometallics* 18 (1999) 709;  
(b) S. Fernandez, M. Pfeffer, V. Ritleng, C. Sirlin, *Organometallics* 18 (1999) 2390;  
(c) H. Brunner, R. Oeschey, B. Nuber, *J. Chem. Soc., Dalton Trans.* (1996) 1499;  
(d) J.W. Faller, J. Parr, *Organometallics* 19 (2000) 1829.